



Open Archive TOULOUSE Archive Ouverte (OATAO)

OATAO is an open access repository that collects the work of Toulouse researchers and makes it freely available over the web where possible.

This is an author-deposited version published in : <http://oatao.univ-toulouse.fr/>
Eprints ID : 18201

To link to this article : DOI: 10.1109/EMCEurope.2016.7739248
URL : [http://dx.doi.org/ 10.1109/EMCEurope.2016.7739248](http://dx.doi.org/10.1109/EMCEurope.2016.7739248)

<p>To cite this version : Hairoud Airieau, Siham and Dubois, Tristan and Duchamp, Geneviève and Durier, André <i>Multiport ICIM-CI modeling approach applied to a bandgap voltage reference</i>. (2016) In: EMC Europe 2016, 5 September 2016 - 9 September 2016 (Wroclaw, Poland).</p>
--

Any correspondence concerning this service should be sent to the repository administrator: staff-oatao@listes-diff.inp-toulouse.fr

Multiport ICIM-CI modeling approach applied to a bandgap voltage reference

S. HAIROUD AIRIEAU^{1,2}, T. DUBOIS¹, G. DUCHAMP¹, A. DURIER²

¹ Univ. Bordeaux Lab. IMS, 351 Cours de la Libération, 33400 Talence, siham.hairoud-airieau@ims-bordeaux.fr

² IRT SAINT EXUPERY, 118 Route de Narbonne, 31432 Toulouse, siham.hairoud-airieau@irt-saintexupery.com

Abstract—This paper presents a modeling approach to build a multiport ICIM-CI model describing the impact of RF disturbances injection through different pins of a micro-power bandgap reference. The component chosen for this study is a commercial one. It combines high accuracy and low drift with low supply current and small package.

Keywords—EMC/EMI; Immunity measurement; Immunity modelling;

I. INTRODUCTION

The continuous technological evolutions of integrated circuits (such as complexity and miniaturization), and integration processes (lithography) lead designers to be seeking for new modeling methods to anticipate EMC/EMI (Electro-Magnetic Compatibility/Electromagnetic Interferences) problems, and, to avoid additional post-production costs, while providing both functional and successful circuits. Numerous techniques have thus emerged to increase the immunity of circuits against electromagnetic disturbances, as shown in [1]-[4], to name a few. However, embedded systems should face environmental stress, such as temperature and humidity, which can affect their reliability over their lifetime including their EMC/EMI characteristics [5]-[7]. In that context, ROBUSTESSE-CEM [8] project intends to handle the evolution of the robustness of embedded systems used in avionics, automotive and space equipment. The main objective of this project is to develop predictive models to assure long term EMC compliance of electronic equipment. One of the objectives is then to improve the ICIM-CI model (Integrated Circuit Immunity Model Conducted Immunity) in order that it can take into account the effect of aging in the immunity characteristics of electronic components.

The aim of this paper is to present the methodology to build a multiport ICIM-CI behavioral model of a bandgap voltage reference, before starting the aging process. This one takes into account the variation of the V_{dd} supply and the current load. The model is fed by empiric parameters. It is developed and validated thanks to DPI (Direct Power Injection) measurements. The simulated and measured immunity levels are then compared and analyzed.

After a brief description of the ICIM-CI model in section II, section III presents the characteristics of the considered DUT and PCB. Section IV introduces the measurement setup and

methods used to extract the influent parameters. Section V presents in details the approach followed to develop and to validate the model. The conclusions and perspectives are finally exposed in section VI.

II. ICIM-CI MODEL DESCRIPTION

As it is presented in the standard IEC 62433-4 [9], the ICIM-CI model is composed of two blocks: the PDN (Passive Distribution Network), and the IB (Internal Behavioral). The model output is then compared to an application-dependent user-definable threshold.

A. PDN (Passive Distributed Network)

The PDN block describes the impedance network of one or more IC ports with passive elements (resistors, capacitors, inductors). The equivalent impedance measurements should be carried out in the standard operating conditions [9]. The experimental set-up dedicated to the conducted immunity measurements is presented in section III. Note that the PDN is defined in the frequency domain and can have various descriptions such as S- or Z- or Y-parameters.

B. IB (Internal Behavioral)

The IB block represents the active part of a device and characterizes the device dysfunction due to electromagnetic disturbance. The IB observable output describes the IC behavioral response to a disturbing signal applied to the IB block input, in other words, how ICs react to internal disturbances [9].

C. Immunity criterion

The Immunity criterion is applied to the observable output of the IB block and is currently fixed by the IC model user. The choice of the immunity criterion should be done in accordance with the application in which the IC is used [9].

D. ICIM-CI modeling approach

As for the model described in the standard IEC 62433-4 [9], the new ICIM-CI model proposed in this paper (Fig. 1) is composed of PDN and IB blocks. In this study case, the PDN model describes all the S-parameters and each IB model corresponds to one injection port. The DI (Disturbance Input) corresponds to the input terminal for the RF disturbances injection and the OO (Observable Output) corresponds to the output terminal where the immunity criterion is applied.

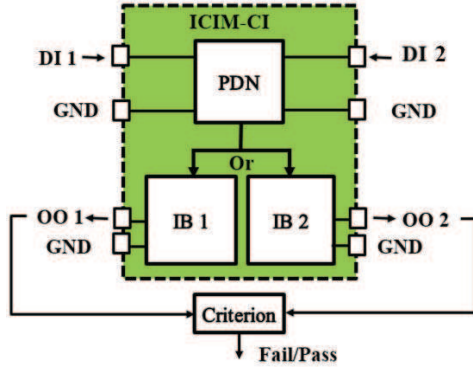


Fig. 1. ICIM - CI model

III. DESCRIPTION OF THE DEVICE UNDER TEST AND THE DEMONSTRATOR

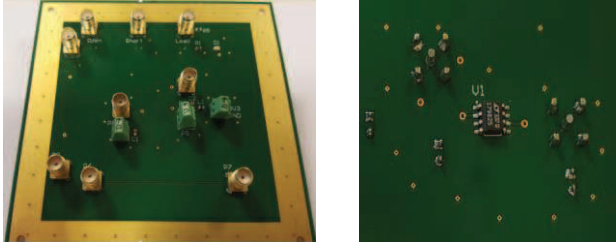
This part of the paper gives an overview of the considered device under test and the electronic board used as demonstrator.

A. LTC1798-2.5V characteristics

The LTC1798-2.5V is a micro-power bandgap reference from Linear Technology. It combines high accuracy and low drift ($\pm 0.15\%$) with very low supply current and small package. An input decoupling capacitor and an output bypass capacitor of $0.1 \mu\text{f}$ are used for stability reasons. This component is guaranteed functional over the operating temperature range of 0°C to 70°C and supplies a $2.5 \text{ V} \pm 3.7 \text{ mV}$ output voltage as far as V_{dd} varies from 2.7 V to 12.6 V .

B. Demonstrator characteristics

The PCB presented in Fig. 2, on which the tested component is soldered, has 4 layers with an overall thickness equal to 1.6 mm . The material used is the standard FR4.



a) Bottom side b) Top side
Fig. 2. ELECIS-V demonstrator

IV. DESCRIPTION OF MEASUREMENTS

A. DPI (Direct Power Injection) measurements

The DPI measurements were carried out by injecting an interference signal through a bias tee connected to the V_{dd} pin (input pin) or to the V_{out} pin (output pin). Fig. 3 presents the injection configurations. It is well understood that the case where the interference is injected to the input and output pin at the same time is not addressed in this study.

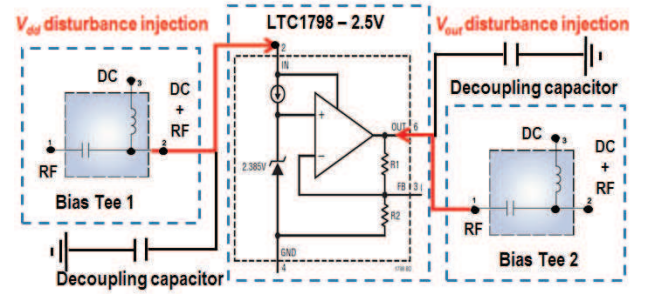


Fig. 3. LTC1798-2.5V block diagram + bias tees

As in the ICIM-CI standard proposal [9], we have to quantify the power that induces a device dysfunction. The transmitted power P_{trans} absorbed by the tested component is considered as a relevant parameter to characterize the signal drift at the observable output (Fig. 1). It is deduced from forward and reverse powers (P_{forw} and P_{rev} , respectively) as shown by equation (1).

$$P_{trans} = P_{forw} - P_{rev} \quad (1)$$

Note that P_{forw} and P_{rev} are measured from the bidirectional coupler with a power meter (Fig. 4). Note that, the forward and reverse powers measured at the coupler (J_3 and J_4 , respectively) level are different from the forward and reverse powers present right at the DUT DI input. These differences come from the signal attenuation caused by the test fixtures (the bidirectional coupler, the coaxial cable and the bias tee).

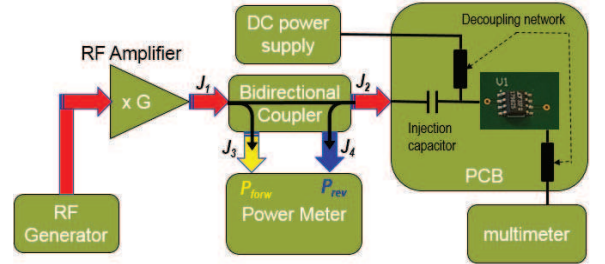


Fig. 4. Illustration of the DPI setup

The cascaded S-parameters network composed by the identified test fixtures (the bidirectional coupler, the coaxial cable and the bias tee) is computed. Fig. 5 shows that the transmission coefficient S_{21} between the coupler input and the DUT disturbance input varies from -0.4 to -2 dBm .

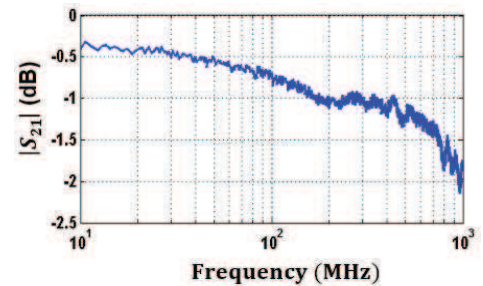


Fig. 5. S_{21} parameter - cascaded network (coupler, coaxial cable and bias tee)

The quantification of the signal losses in the test fixtures allows us precisely determining the forward power at the DI input of the DUT. Once all the losses are taken into account, the transmitted power (power absorbed by the voltage reference) is then deduced thanks to equation (2) (DI through V_{dd}) or equation (3) (DI through V_{out}):

$$P_{trans\ Vdd} = P_{forw\ Vdd} * (1 - |S_{11}|^2) \quad (2)$$

$$P_{trans\ Vout} = P_{forw\ Vout} * (1 - |S_{22}|^2) \quad (3)$$

The S_{11} and the S_{22} parameters are obtained by measuring the S-parameters of the polarized DUT (V_{dd} supply equal to 3.3 V). More explanation will be given in the subchapter IV-D. Fig. 6 and Fig. 7 give the DPI results obtained when the RF disturbances are injected respectively through V_{dd} and V_{out} pins, considering the power absorbed by the component directly measured by the power meter and computed right at the input of the component. For this measurement, the component is considered disturbed (immunity criterion) if its output voltage shifts of -5 mV from its nominal value equal to 2.5 V, corresponding to an error of 0.2%. Consequently, Fig. 6 and Fig. 7 give an idea of the measurement error made if the DPI test fixtures are not taken into account. We note an important difference of about 8 dB in the first case (Fig. 6) and about 5 dB (Fig. 7) in the second case.

Moreover, it is interesting to observe that the DPI results in both cases show the highest susceptibility of the LTC1798-2.5V component in the frequency bandwidth from 100 MHz to 400 MHz. In this frequency range, a weak disturbance signal (about -20 dBm) can drift the observable output (V_{out}) of -5 mV.

Note that for the case where the disturbances are injected through the V_{dd} pin, the immunity criterion still unreachable for frequencies values from 10 MHz to 70 MHz, because of the amplifier power limit.

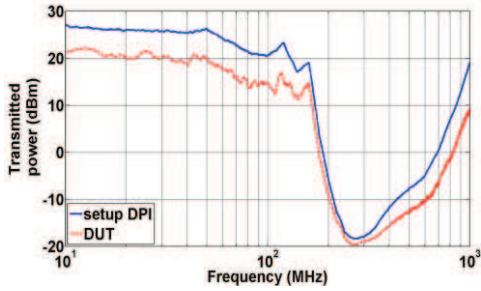


Fig. 6. Transmitted power (dBm) – V_{dd} pin

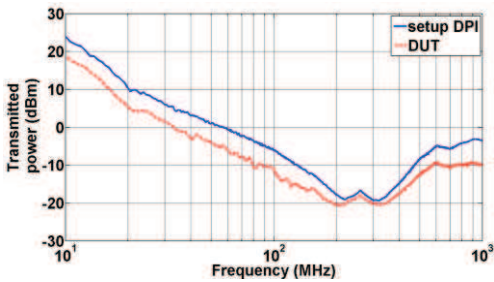


Fig. 7. Transmitted power (dBm) – V_{out} pin

B. Effect of the load current change on the DPI measurement

The LTC1798-2.5V output can source up to 10 mA. Different loads values, greater than 250 Ω were used, so that, the current load remains below to 10 mA. The DPI measurements were carried out for 270 Ω , 470 Ω , 1 k Ω , 10 k Ω , 100 k Ω and 330 k Ω . Fig. 8 shows how the immunity of the component can change depending on the load value. For different frequencies values, we notice that, the “weak values” of loads (270 Ω , 470 Ω and 1 k Ω) degrade the immunity of the component, while the “high values” of loads seem to not affect the immunity of this last one. The model presented in this paper is valid for loads values greater than 10 k Ω .

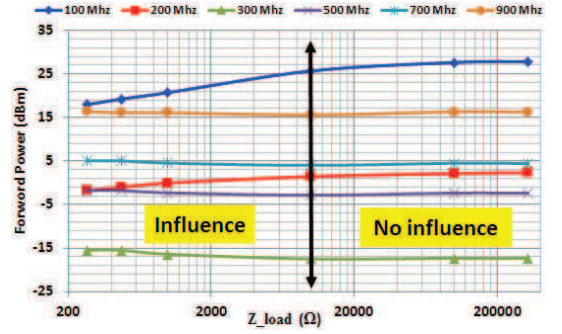


Fig. 8. Effect of the current load change on forward power

C. Effect of V_{dd} supply change on the DPI measurement

The LTC1798-2.5V can supply a 2.5 V output voltage as far as V_{dd} varies from 2.7 V to 12.6 V. The DPI measurements were carried out for V_{dd} equals to 3.3 V, 6.3 V, 9.3 V and 12.3 V. Fig. 9 shows the forward power obtained for different V_{dd} supplies and frequencies. Except for the measurements performed at 200 MHz, the V_{dd} supplies seem to have a weak effect on the DPI measurements.

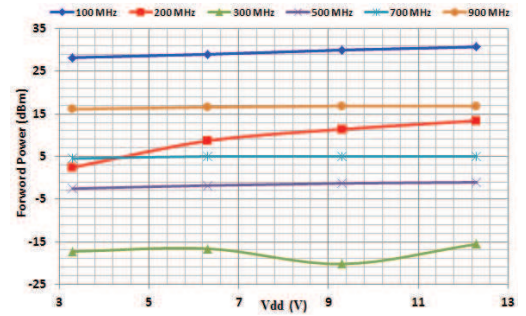


Fig. 9. Effect of V_{dd} change on forward power

D. Effect of polarization on the S-parameters measurement

The PDN block describes the impedance network of two IC ports (V_{dd} and V_{out}). The S-parameters measurements have been performed between V_{dd} and V_{out} pins. Here, we focus on two cases. In the first case, the S-parameters are measured when the DUT is non-polarized. In the second case, the S-parameters are measured when the DUT is polarized (V_{dd} equal to 3.3V). The results are presented in Fig. 10 and show a difference between these two cases, especially for the transmission coefficients where a difference about 2 dB was

noticed from 100 MHz to 400 MHz. Therefore, the PDN will be built using the S-parameters obtained when the DUT is polarized.

V. ICIM-CI MODEL

A. PDN construction

The PDN is built using the ADS simulation tool. Fig. 11 shows the multiport PDN equivalent electrical schematic. This one models the SMA connectors, the decoupling capacitors, the interconnections of the PCB as well as Z_{in} and Z_{out} corresponding respectively to the input and output impedance of the tested component. Fig. 12 presents the S-parameters of the DUT obtained by measurement and by simulation (dashed curves). A very good agreement is obtained for all the four S-parameters. Let's precise, the difference observed on S_{12} and S_{21} parameters at low frequency is due to measurement limitations.

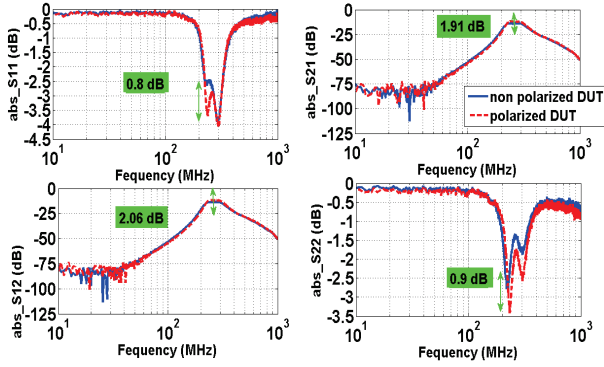


Fig. 10. Effect of polarization on S-parameters

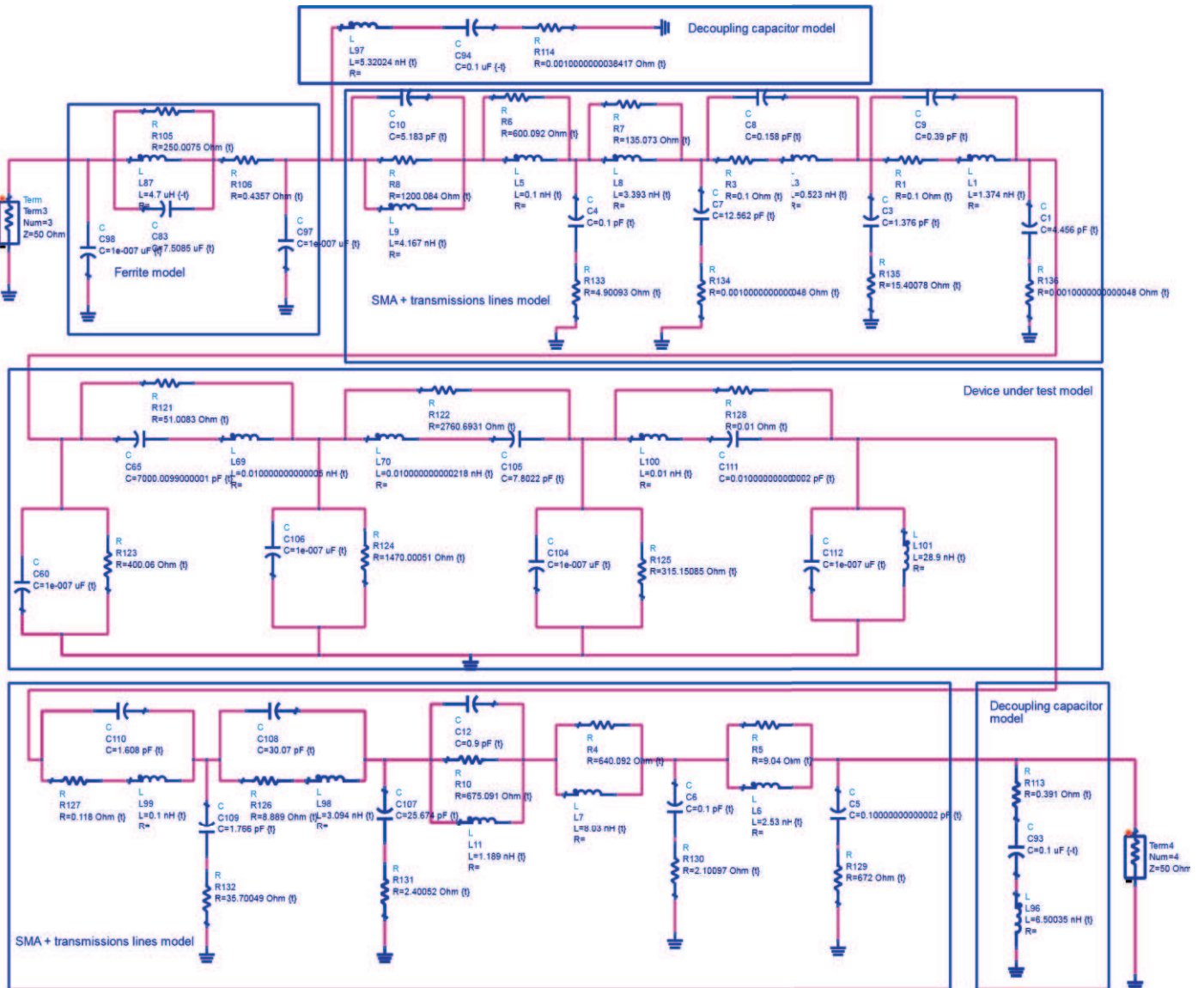


Fig. 11. PDN electrical schematic

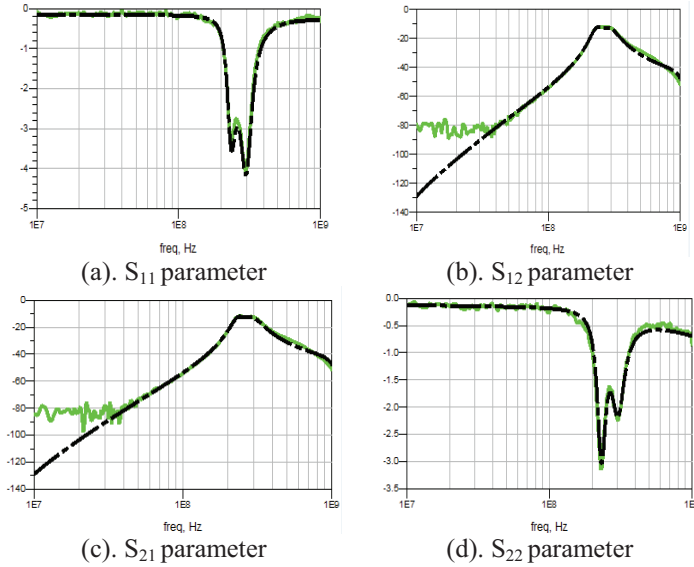


Fig. 12. S-parameters comparison between simulations and measurements

B. IB Model construction - RF injection on V_{dd}

The aim of this part of the study is to determine a mathematical equation describing the immunity behavior of the component when an interference signal is injected at the input and the output of the tested component. In order to define this equation, several DPI measurements are performed. The first step consists in determining the functions $V_{out}(P_{forw_Vdd})$ and $V_{out}(P_{forw_Vout})$ for different frequencies. Let focus on $V_{out}(P_{forw_Vdd})$. The reference voltage output (V_{out}) is measured for different forward powers values from -20 to 15 dBm. The same measurements have been repeated for 34 frequencies comprised between 10 MHz and 1 GHz. Fig. 13 presents V_{out} as a function of P_{forw_Vdd} for a frequency of 800 MHz. We notice that V_{out} is linearly dependent on the forward power (P_{forw}). The forward power is expressed in Watt. The same observation has been done for every measured frequency. It can be shown that the slop of the linear function depends on the frequency.

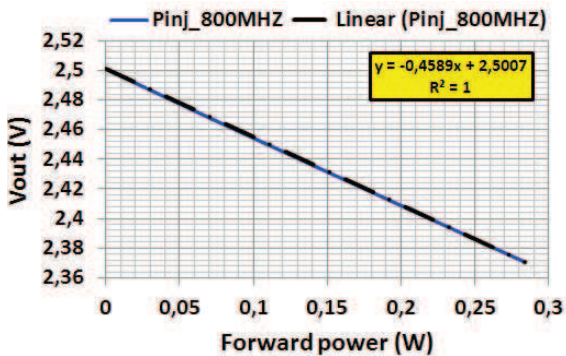


Fig. 13. V_{out} vs P_{forw} - at 800 MHz

Consequently, V_{out} can be expressed by equation (4) where $c_{in}(f)$ corresponds to the slop of the linear function. Here, V_{ref} is fixed to 2.5 V. Fig. 14 presents c_{in} as a function of the frequency. It is interesting to note a similar tendency between the coefficient c_{in} and the S_{11} parameter (Fig. 12(a)).

$$V_{out}(f, P_{forw}) = V_{ref} + c_{in}(f) * P_{forw} \quad (4)$$

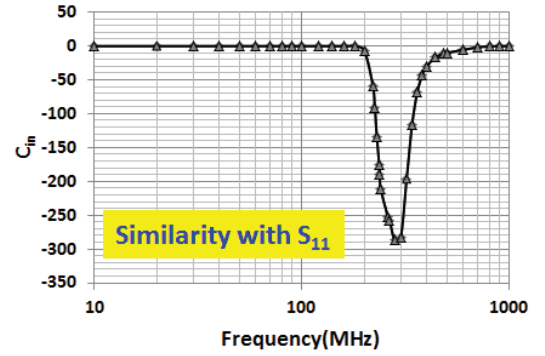


Fig. 14. c_{in} vs frequency

Once this equation is defined, it can be used to generate the evolution of V_{out} as a function of the forward power and frequency. The transmitted power can be computed thanks to the S_{11} parameter and to the forward power. Finally, it is possible to plot the immunity curve of the component for a given immunity criterion.

Fig. 15 shows the comparison between the forward and transmitted (absorbed) power necessary to reach an immunity criterion of -5 mV, obtained by measurement and simulation at the DUT level. A very good correlation between measurement and simulation is obtained, validating the model.

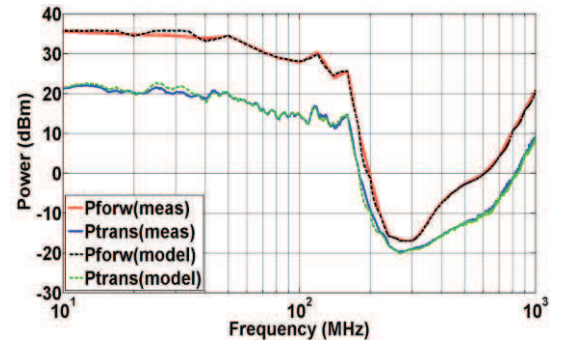


Fig. 15. Comparison between measurements and model simulations at DUT level (at J2 port (Fig. 4))

C. IB Model construction - RF injection on V_{out}

The same processes are performed to determine $V_{out}(P_{forw_Vout})$ with the RF interference signal injected through V_{out} pin. Fig. 16 presents V_{out} as a function of P_{forw_Vout} for a frequency of 800 MHz.

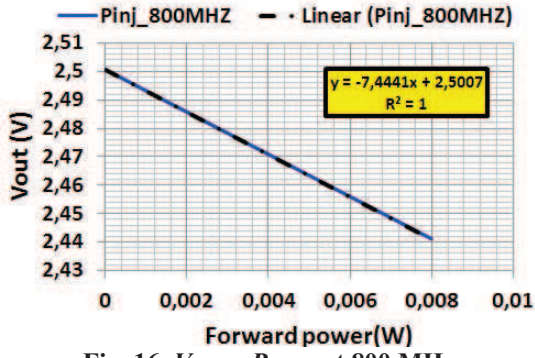


Fig. 16. V_{out} vs P_{forw} - at 800 MHz

$$V_{out}(f, P_{forw}) = V_{ref} + c_{out}(f) * P_{forw} \quad (5)$$

As for the previous example, Fig. 16 shows that V_{out} is linearly dependent on the forward power. So, V_{out} is expressed by forward power following the equation (5). V_{ref} is still fixed to 2.5V. The coefficient c_{out} is extracted for each frequency (Fig. 17). As for the c_{in} coefficient, it is interesting to observe a strong similarity between the coefficient c_{out} (Fig. 17) and the parameter S_{22} (Fig. 4 (d)).

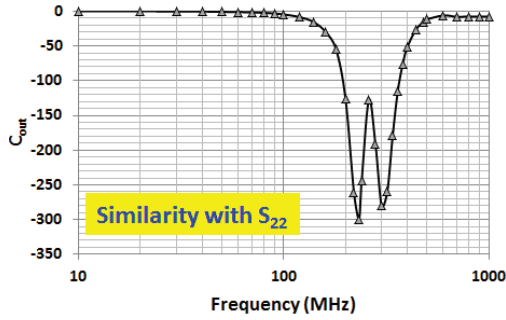


Fig. 17. c_{out} vs frequency

The model is finally used to determine the immunity curve when interference is injected at the output of the component for an immunity criterion of - 5 mV. Fig. 18 shows that the model curves fit very well the measurement curves.

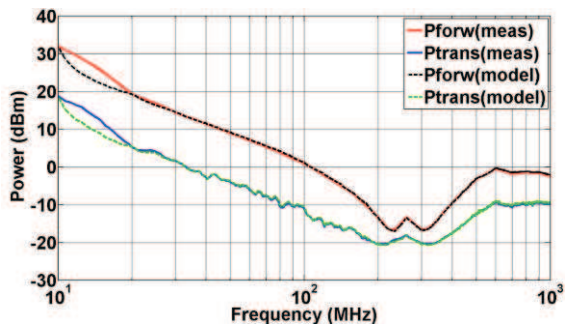


Fig. 18. Comparison between measurements and model at DUT level

VI. CONCLUSION

In conclusion, this study focuses on the immunity of a micro-power bandgap reference from Linear Technology.

The disturbances signals are injected successfully through the V_{dd} and V_{out} pins. The component is more susceptible in the case where disturbances are injected through V_{out} pin. The characterization of the DPI setup shows that the test fixtures losses can induce non-negligible errors in the different measured power if they are not taking into account. The effects of variation of the V_{dd} supply and the current load on the immunity of the component have been studied. The methodology followed to build the ICIM-CI model for all the component terminals has been presented. At the end, the complete ICIM-CI model of the tested component is composed of a unique multiport PDN associated with two IB blocks. It describes the component immunity behavior when interferences are injected at its input or at its output. Good agreement has been obtained between measurements and simulations, validating the multiport ICIM-CI model.

References

- [1] Pelliconi, R., Speciale, N., "Criteria to reduce failures induced by EMI conducted on the power supply rails of CMOS operational amplifiers," *Electromagnetic Compatibility, 2001. EMC. 2001 IEEE International Symposium*, vol. 2, pp. 1102, 1105, 2001.
- [2] Fiori, F., "Operational amplifier input stage robust to EMI", *Electronics Letters*, vol. 37, no. 15, pp. 930-931, 2001.
- [3] M. Ramdani & al.; "The Electromagnetic Compatibility of Integrated Circuits - Past, Present, and Future" *IEEE Transactions on Electromagnetic Compatibility*, vol.51, pp.78-100, 2009.
- [4] E. Sicard, S. B. Dhia, M. Ramdani, J. Catrysse, and M. Coenen, "Towards an EMC roadmap for integrated circuits"; presented at the *Electromagn. Compat. EMC- Compo.*, 2007, Torino, Italy.
- [5] R. Fernandez, I. Gil, "Impact of Temperature on the Electromagnetic Susceptibility of Operational Amplifiers", *Progress in Electromagnetics Research Symposium*, pp. 1063-1065, 2012.
- [6] H. Huang, A. Boyer, S. Ben Dhia, B. Vignon, "Prediction of Aging Impact on Electromagnetic Susceptibility of an Operational Amplifier", *Asia-Pacific International EMC Symposium 2015*, p. 4, May 2015.
- [7] T. Dubois, S. Hairoud, M. H. Gomes de Oliveira, H. Frémont et G. Duchamp, "Characterization and model of temperature effect on the conducted immunity of Op. Amp", *Microelectronics Reliability*, doi:10.1016/j.microrel.2015.06.0182015, 2015.
- [8] Durier, A., Boyer, A., Duchamp, G., "A methodologic project to characterize and model COTS components EMC behavior after ageing", *APEMC proceeding 7th Asia-Pacific International Symposium*, 2016.
- [9] IEC 62433-4: integrated circuit - EMC IC modeling – Part 4: Models of Integrated Circuits for EMI behavioral simulation, Conducted Immunity Modeling (ICIM-CI). IEC standard proposal, 2008.
- [10] IEC 61967-1: Integrated circuits – Measurement of electromagnetic emissions, 150 kHz to 1 GHz - Part 1: General conditions and definitions, 2002.